

# Intracellular trafficking pathway of newly synthesized CD1b molecules

V. Briken, R.M. Jackman, S. Dasgupta<sup>1</sup>,  
S. Hoening<sup>2</sup> and S.A. Porcelli<sup>3</sup>

Department of Microbiology and Immunology, Albert Einstein College of Medicine, Bronx, NY 10461, <sup>1</sup>Department of Biochemistry & Biophysics, University of California, San Francisco, CA 94143-0534, USA and <sup>2</sup>Georg-August University, Gosslerstrasse 12d, D-37073 Göttingen, Germany

<sup>3</sup>Corresponding author  
e-mail: porcelli@aecom.yu.edu

**The intracellular trafficking of major histocompatibility complex (MHC) class I and class II molecules has evolved to support their function in peptide antigen presentation optimally. We have analyzed the intracellular trafficking of newly synthesized human CD1b, a lipid antigen-presenting molecule, to understand how this relates to its antigen-presenting function. Nascent CD1b was transported rapidly to the cell surface after leaving the Golgi, and then entered the endocytic system by internalization via AP-2-dependent sorting at the plasma membrane. A second sorting event, possibly involving AP-3 complexes, led to prominent accumulation of CD1b in MHC class II compartments (MIICs). Functional studies demonstrated the importance of nascent CD1b for the efficient presentation of a foreign lipid antigen. Therefore, the intracellular trafficking of nascent CD1b via the cell surface to reach MIICs may allow the efficient sampling of lipid antigens present in endocytic compartments.**

**Keywords:** adaptor protein complex/antigen presentation/CD1/dendritic cells/MIIC

## Introduction

The CD1 cell surface glycoproteins are now well established as a third distinct family of antigen-presenting molecules that have the unique capacity to bind lipid ligands and present them to T cells (Porcelli, 1995). The human group I CD1 proteins, consisting of CD1a, CD1b and CD1c isoforms, have been shown to present lipids and glycolipids from mycobacteria to T cells belonging to a variety of different phenotypic subsets (Burdin and Kronenberg, 1999; Porcelli and Modlin, 1999). In addition, T-cell responses to a CD1c-presented mycobacterial isoprenoid glycolipid antigen have been shown to be elevated in the blood of human subjects previously infected with *Mycobacterium tuberculosis* (Moody *et al.*, 2000). These findings underscore the potential importance of antigen presentation by the CD1 system in the immune response to pathogens.

CD1a, -b and -c isoforms are expressed by lymphoid and myelomonocytic cells, with the most prominent

expression occurring on myeloid lineage dendritic cells (DCs) (Porcelli, 1995). Recent studies have characterized the intracellular localization of different CD1 isoforms as overlapping but not identical. Whereas CD1a and CD1c accumulate at the cell surface and in early endosomes (Sugita *et al.*, 1999; Briken *et al.*, 2000a), CD1b and murine CD1d are found mainly in late endosomes, lysosomes and major histocompatibility complex (MHC) class II compartments (MIICs) (Sugita *et al.*, 1996; Chiu *et al.*, 1999). These results support the hypothesis that the evolution and conservation of different CD1 isoforms may be due at least in part to their ability to survey the lipid content of different intracellular compartments efficiently (Briken *et al.*, 2000b). Most CD1 proteins contain a tyrosine-based motif (YXXZ) in their short cytoplasmic tails (Jackman *et al.*, 1998). These YXXZ motifs (Y is a tyrosine, X is any amino acid and Z is a bulky hydrophobic amino acid) interact with cytosolic adaptor protein (AP) complexes to induce sorting into transport vesicles (Kirchhausen *et al.*, 1997; Bonifacino and Dell'Angelica, 1999).

Knowledge of the intracellular transport of antigen-presenting molecules has provided important information about the molecular mechanisms by which they function. Thus, examination of the transport of MHC class I molecules revealed that the rate-limiting step of their cell surface appearance was the transport from the endoplasmic reticulum (ER) to the Golgi apparatus. From the Golgi, MHC class I proteins traffic rapidly to the plasma membrane (PM) where they accumulate, since internalization from the cell surface is inefficient. These results were consistent with experiments showing loading of the MHC class I proteins with antigenic peptides in the ER (Germain and Margulies, 1993; Heemels and Ploegh, 1995; Pamer and Cresswell, 1998). In contrast, the intracellular transport of MHC class II molecules is characterized by their sorting at the *trans*-Golgi network (TGN) for transport to the endocytic pathway where MHC class II molecules reside for 2–3 h, to allow degradation of their associated invariant chain (Ii chain) and binding to antigenic peptides, before reaching the cell surface (Mellman *et al.*, 1995; Pieters, 1997). Internalization and recycling of MHC class II from the cell surface is inefficient but nevertheless represents a minor alternate pathway for MHC class II peptide loading (Pinet *et al.*, 1995).

CD1b molecules mainly accumulate in lysosomes and MIICs in immature dendritic cells (iDCs), which is very similar to the intracellular distribution of MHC class II molecules (Sugita *et al.*, 1996; Briken *et al.*, 2000a). However, the transport pathway that newly synthesized CD1b molecules employ to reach MIICs remains to be elucidated. In this study, we analyzed the trafficking of newly synthesized CD1b molecules to determine the route

that these take to reach lysosomal compartments where they are most efficiently loaded with lipid antigens. Our results showed that CD1b molecules have evolved an unusual intracellular trafficking pathway that is unlike those previously found for MHC class I or class II antigen-presenting molecules, and suggest that this is likely to be essential to the unique function of CD1b in the binding and presentation of lipid antigens throughout the endocytic pathway.

## Results

### Direct transport of CD1b from the Golgi apparatus to the cell surface

To study the intracellular transport of CD1b, the human B-lymphoma cell line C1R stably transfected with CD1b was used. To validate the use of these cells as a model for intracellular trafficking of CD1b, the steady-state distribution of CD1b in iDCs and C1R cells was compared by confocal immunofluorescence microscopy using Lamp-1 as a marker of late endosomes and lysosomes (Figure 1A). In addition, the distribution of CD1b in fractions of total cellular membranes separated on Percoll gradients was compared for iDCs and C1R cells (Figure 1B) (Briken *et al.*, 2000a). With both methods, the steady-state distribution of CD1b molecules was very similar in iDCs and C1R cells, indicating similar intracellular trafficking of CD1b in these cells.

To determine whether the transport of newly synthesized CD1b molecules followed the pathway of secretory molecules or instead a pathway resembling that of MHC class II molecules, pulse-chase experiments were performed using C1R cells transfected with CD1b or HLA-A3. First, the cell surface appearance of MHC class II molecules was analyzed, serving as an example of a molecule that enters the endocytic pathway after passing through the Golgi apparatus but before reaching the cell surface. The signal of the total MHC class II  $\alpha$ -chain precipitated remained constant from 1 to 6 h of chase. The cell surface signal of the MHC class II  $\alpha$ -chain was weak after 1 and 2 h of chase, but strongly increased after a 4 h chase, with a further slight increase at 6 h of chase (Figures 2A and 3). This delay in surface expression is known from previous studies to be due to the transport of MHC class II into the endocytic pathway, where the catabolism of the Ii chain and loading with antigenic peptides occurs, before the appearance of newly synthesized MHC class II complexes at the cell surface (Mellman *et al.*, 1995).

As examples of proteins that follow the secretory pathway and that are directly transported to the cell surface after leaving the Golgi, the intracellular transport of transferrin receptor (TfR) and MHC class I was analyzed (Neefjes *et al.*, 1990). For this analysis, the immunoprecipitated proteins were treated with endoglycosidase H (EndoH) before separation by SDS-PAGE, in order to differentiate between proteins in the ER and the Golgi apparatus. This allowed measurement of the kinetics of the Golgi to cell surface transport without any influence of the ER to Golgi transport, which may otherwise also account for a delay in the cell surface appearance of a protein. This distinction was not necessary for the analysis of MHC class II molecules described above, since the rate-limiting

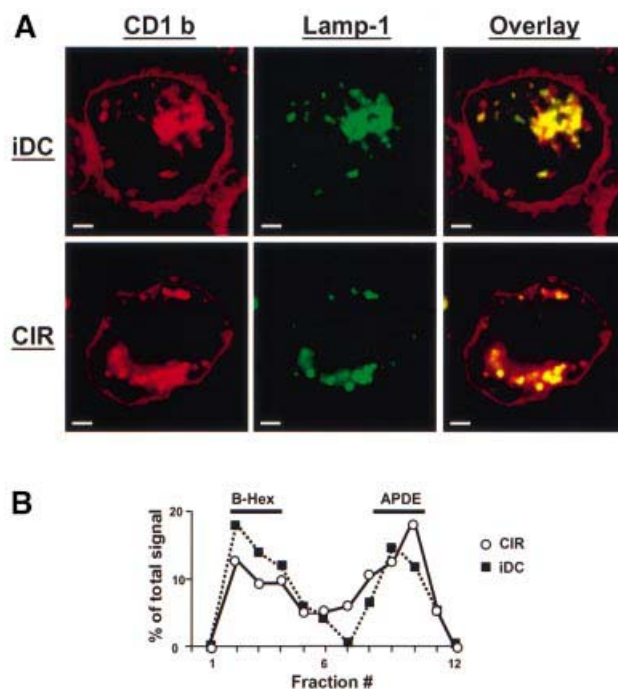


**Fig. 1.** Similar steady-state distribution of CD1b in iDCs and CD1b-transfected B lymphoblastoid cells. (A) The distribution of CD1b in either iDCs (top row) or CD1b-transfected C1R cells (bottom row) was analyzed by immunofluorescence and confocal microscopy. Single channel images show CD1b staining (BCD1b3.1) in red (left column) and Lamp-1 staining (rabbit anti-Lamp1 serum) in green (middle column). Co-localization of the two proteins is revealed as yellow staining in the overlay of the two scanned images (right column). Scale bar: 2  $\mu$ m. (B) Lysosomal compartments of C1R cells or iDCs were separated from endosomes and the plasma membrane using Percoll gradients. The distribution of CD1b in the fractions of each gradient is shown as a percentage of the total signal of CD1b in each gradient as described in Materials and methods. The quality of the separation was similar for each gradient, as controlled by the distribution of the lysosomal and plasma membrane marker enzymes  $\beta$ -hexosaminidase (B-Hex) and alkaline phosphodiesterase (APDE), respectively (Briken *et al.*, 2000a).

step of the cell surface transport for these molecules has been shown previously to be their exit from the endocytic pathway (Neefjes *et al.*, 1990).

After 1 h, ~30% of the total HLA-A3 molecules were resistant to EndoH digestion and this signal remained constant thereafter, although the EndoH-sensitive signal decreased, most probably due to maturation and/or degradation (Figure 2B). After 1 h of chase, only a small fraction of HLA-A3 was found at the cell surface, but after 2 h most of the molecules (~80%) had reached the cell surface with only a minor further increase at subsequent time points (Figures 2B and 3). Parallel analysis of the TfR also showed that its transport to the cell surface from the Golgi was very rapid, since after 1 h of chase the maximal amount of TfR molecules was found at the cell surface and thereafter slowly decreased until it equilibrated at ~70% of the maximal level (Figures 2C and 3). The significantly lower plateau of cell surface signal of the TfR (~70%) compared with MHC class I (~100%) most probably reflected the higher internalization and recycling rates of the TfR.

Using the same approach, the cell surface transport of newly synthesized CD1b molecules was also analyzed

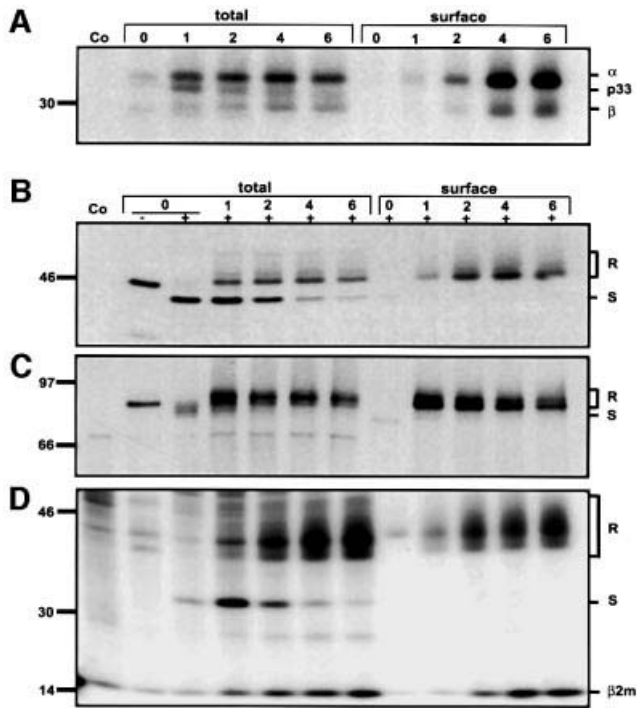


**Fig. 2.** Rapid trafficking of newly synthesized CD1b from the Golgi apparatus to the cell surface. The cell surface arrival of newly synthesized MHC class II (A), MHC class I (B), Tfr (C) and CD1b (D) was compared by pulse labeling of C1R cells, followed by the indicated chase periods. The 'total' and 'surface' fractions of newly synthesized proteins were determined as described in Materials and methods. For (B–D), the proteins were subjected to EndoH digestion to differentiate between proteins in the ER or the Golgi and post-Golgi compartments. The sizes of EndoH-resistant and EndoH-sensitive proteins are indicated on the right by an 'R' or 'S', respectively. For (A), the sizes of the MHC class II  $\alpha$ - and  $\beta$ -chains and the associated invariant chain (p33) are indicated. The experiment shown is representative of four independent experiments.

(Figures 2D and 3). It was apparent from the relative levels of EndoH-sensitive and -resistant CD1b during the chase period that the transit of CD1b molecules from the ER to the Golgi was significantly slower than that of HLA-A3 and Tfr. Thus, even after 2 h of chase, the amount of EndoH-resistant CD1b still strongly increased, and after 4 h of chase there was still a small increase of signal (Figure 2D). However, the increase in EndoH-resistant material was paralleled by a simultaneous increase in cell surface expression at each time point. For example, the strongest increase of EndoH-resistant signal in the total immunoprecipitate was observed between 1 and 2 h of chase, and this was also the interval in which the greatest increase in the cell surface signal of CD1b occurred (Figures 2D and 3). Thus, unlike MHC class II molecules, CD1b molecules that had reached the Golgi apparatus were rapidly transported to the cell surface with kinetics intermediate between those of the Tfr and MHC class I (Figure 3). This indicated that the majority of newly synthesized CD1b molecules were not delayed in their movement to the cell surface by transit through endosomes and lysosomes as observed for MHC class II, but instead were transported directly to the cell surface after leaving the Golgi via the secretory pathway.

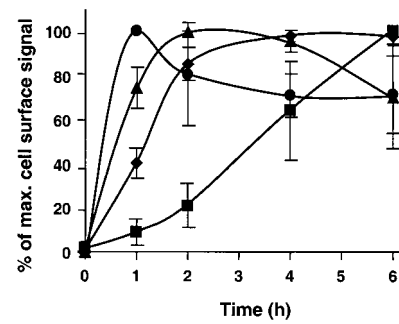


**Fig. 3.** Quantification of Golgi to cell surface transport of CD1b, Tfr and MHC class I and II. The appearance of newly synthesized CD1b (triangles), Tfr (circles), MHC class I (diamonds) and MHC class II (squares) as analyzed in Figure 2 was quantified using either a Phosphoimager (two experiments) or densitometry (two experiments). For MHC class II, the signal of the  $\alpha$ -chain in the 'total' immunoprecipitation (IP) was compared with the signal in the 'surface' IP. For all the other molecules, only the fraction of EndoH-resistant signal in the 'total' was compared with the 'surface' IP in order to eliminate any influence of the kinetics of the ER to Golgi transport in determining the kinetics of cell surface appearance. The maximal amount of cell surface signal for each molecule was normalized and set to 100% to facilitate comparison of the kinetics of cell surface arrival between all molecules.

#### **Clathrin-mediated endocytosis of CD1b molecules from the cell surface**

Since newly synthesized CD1b molecules accumulate in late endosomes and MIICs, but appeared not to enter these compartments directly upon leaving the Golgi, we hypothesized that this resulted from efficient internalization of CD1b molecules from the cell surface. The internalization of CD1b, Tfr and MHC class I was determined as described in Materials and methods. As expected, the internalization of Tfr was very rapid and efficient, showing ~50% internalization after 10 min. In contrast, at this time point, only ~5% of the MHC class I molecules and 10% of CD1b molecules had been internalized. The internalization of CD1b molecules was less than that of Tfr even at later time points, but was more efficient when compared with MHC class I, since it increased to ~25% after 40 min and 30% after 60 min, whereas the amount of internalized MHC class I remained stable at ~10% at these time points (Figure 4A, left). Internalization of CD1b from the PM was dependent on its cytoplasmic tail, since the rate of internalization of CD1b molecules from which the cytoplasmic tail had been deleted fell to the extremely low level observed for MHC class I (Figure 4A, right).

CD1b molecules previously were shown to localize in clathrin-coated pits at the PM and in clathrin-coated vesicles by immunoelectron microscopy (Sugita *et al.*, 1996). This is believed to be a consequence of the interaction of the YXXZ motif in the CD1b cytoplasmic tail with AP-2 complexes, which then recruit clathrin to the cytoplasmic face of the PM. To verify that the internalization of CD1b was due to interaction with AP-2 and subsequent recruitment of clathrin, the effects of two different dominant-negative mutants of the protein dynamin were tested. Mutation of the lysine residue at position 44 of this protein to alanine (K44A) previously has been demonstrated to inhibit the formation of dynamin oligomers, resulting in a dominant-negative form of

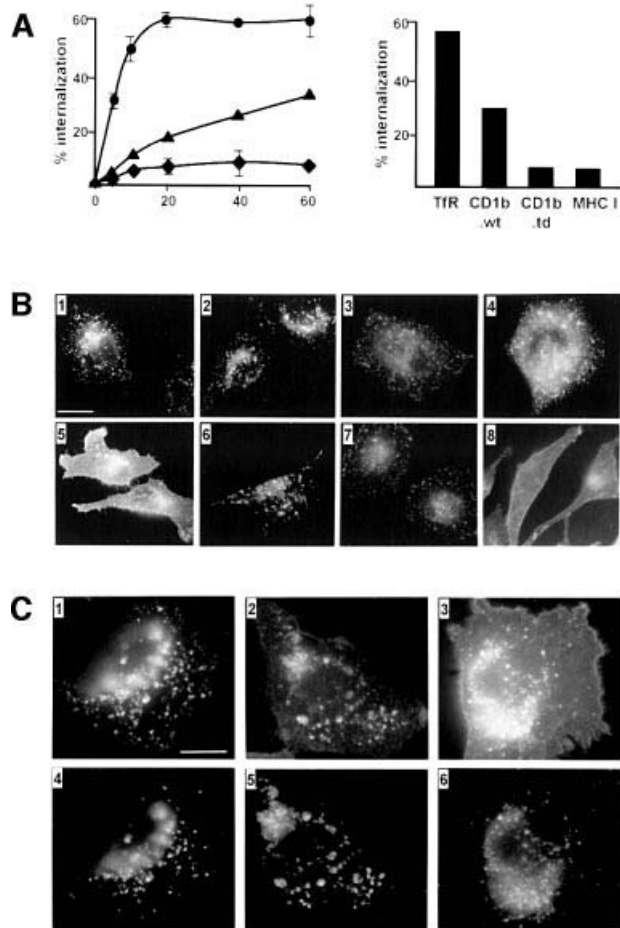


**Fig. 4.** Efficient internalization of CD1b from the cell surface was mediated by AP-2. (A) The internalization kinetics (left panel) of TfR (circles), MHC class I (diamonds) and CD1b (triangles) were analyzed in CD1b-transfected C1R cells using a cell surface biotinylation-based method as described in Materials and methods. The dependence on the cytoplasmic tail of CD1b for internalization was determined using C1R cells transfected either with the wild-type CD1b (CD1b.wt) or with a tail-deleted mutant (CD1b.td). End point internalization of CD1b.wt or CD1b.td after 75 min at 37°C was compared with TfR and MHC class I using an antibody-based internalization assay as described in Materials and methods (right panel). Results shown are means of three independent experiments; the standard deviation is indicated (left panel) or was <4% for any time point (right panel). (B) HeLa cells containing a stably transfected, tetracycline-repressible form of a dominant-negative dynamin mutant (K44A-dynamin) were transiently transfected with CD1b (1 and 5), HLA-DM  $\alpha$ - and  $\beta$ -chains (3 and 7) or mock-transfected with empty vector (2, 4, 6 and 8). Expression of K44A-dynamin was either suppressed in tet<sup>+</sup> medium (1, 2, 3 and 4) or allowed in tet<sup>-</sup> medium (5, 6, 7 and 8) for 48 h. Immunofluorescence staining for CD1b (1 and 5), Lamp-1 (2 and 6), HLA-DM (3 and 7) and TfR (4 and 8) was performed as described (Jackman *et al.*, 1998). (C) HeLa cells expressing the tetracycline-repressible, temperature-sensitive dominant-negative dynamin mutant (G273D-dynamin) were stably transfected with CD1b. Mutant dynamin expression was allowed for 3 days in tet<sup>-</sup> medium at 32°C. Cells were then either fixed (1 and 4), or shifted to the non-permissive temperature of 38°C for 20 min (2 and 5) or 240 min (3 and 6) and analyzed for CD1b (1, 2 and 3) or Lamp-1 (4, 5 and 6) staining. Scale bar: 10  $\mu$ m for all panels in (B) and (C).

dynamin that specifically blocks clathrin-mediated endocytosis at the PM without affecting other intracellular transport steps (Damke *et al.*, 1994; Schmid, 1997). Therefore, the K44A-dynamin mutant also provided an opportunity to dissect further the pathway of CD1b

trafficking by distinguishing AP-2- from AP-1-dependent sorting, thus allowing assessment of the relative importance of the PM-based versus Golgi-based targeting of CD1b to endosomes.

HeLa cells expressing the K44A-dynamin mutant under tight transcriptional regulation by a tetracycline-repressible promoter (Damke *et al.*, 1995a) were transiently transfected with CD1b or HLA-DM ( $\alpha$ - and  $\beta$ -chains). In the presence of tetracycline, the CD1b molecules strongly accumulated in endocytic compartments (Figure 4B) as is normally observed in CD1b-transfected cell lines (Jackman *et al.*, 1998). In contrast, when the K44A-dynamin expression was induced in these cells by shifting them to tetracycline-free medium, the prominent endocytic staining for CD1b was lost and strong cell surface staining was observed (Figure 4B). As controls, we analyzed the localization of HLA-DM and Lamp-1 (which are believed to depend primarily on interactions with AP-1 for lysosomal targeting) and TfR (which uses AP-2 interactions for its internalization and localization to early endosomes) (Bonifacino *et al.*, 1996). As expected, the induction of K44A-dynamin expression did not affect the endosomal expression of HLA-DM and Lamp-1, but induced a strong redistribution of TfR from endosomes to the PM (Figure 4B).

In order to verify these results and analyze the kinetics of the dynamin effect, the temperature-sensitive dominant-negative G273D mutant of dynamin was studied. This mutant functions normally at the permissive temperature (30°C), but converts to a dominant-negative with effects similar to those of K44A-dynamin when shifted to 37°C (Damke *et al.*, 1995b). Cells kept at the permissive temperature showed a characteristic vesicular staining for CD1b and Lamp-1 with no apparent cell surface signal (Figure 4C). After 20 min at the non-permissive temperature, some cell surface staining for CD1b was detected but not for Lamp-1. This difference was more striking after 240 min when a strong signal for CD1b but not for Lamp-1 was found at the cell surface (Figure 4C), consistent with pulse-chase experiments on the kinetics of CD1b transport to the PM (Figure 2). These findings using dominant-negative dynamin mutants provided strong evidence that the majority of the endosomal localization of CD1b resulted from its internalization from the cell surface by a clathrin- and dynamin-dependent mechanism, most probably involving the interaction of AP-2 complexes with the cytoplasmic YXXZ tail motif of CD1b. This contrasted strongly with HLA-DM and Lamp-1 in the same cells, which continued to localize to late endosomes and lysosomes most probably via a dynamin-independent AP-1-mediated sorting to these compartments directly from the TGN.

#### **Measurement of AP-2 and AP-3 binding to the tyrosine-based motif of CD1b by surface plasmon resonance spectroscopy**

The recently identified AP-3 complex is localized on the TGN and on endosomes and has been proposed to have a function in the sorting of proteins in the biosynthetic and endocytic pathways to lysosomes and related organelles (Dell'Angelica *et al.*, 1997, 1999; Simpson *et al.*, 1997; Faundez *et al.*, 1998; Salem *et al.*, 1998). To test the hypothesis that AP-3 may mediate subsequent sorting of

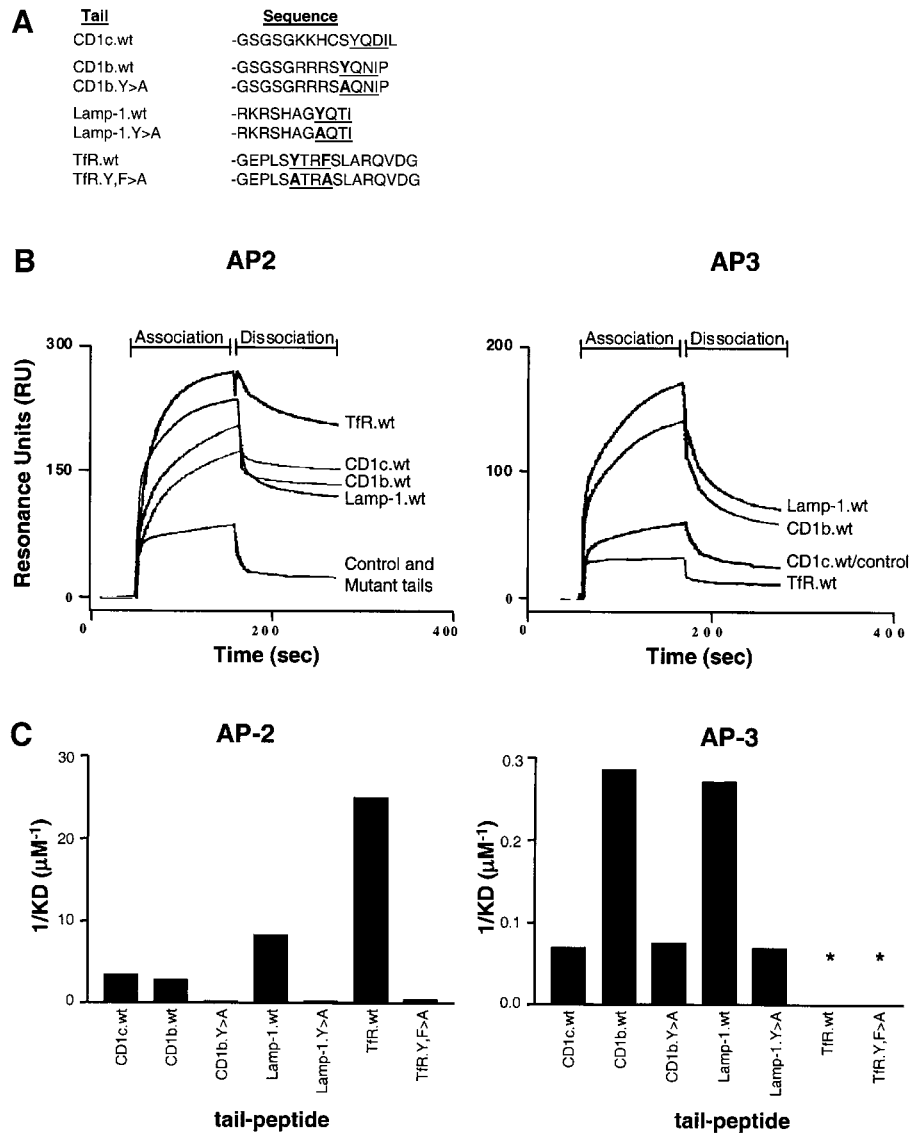


**Fig. 5.** CD1b cytoplasmic tail peptides bind AP-2 and AP-3 complexes. (A) Cytoplasmic tail peptides of Lamp-1, TfR, CD1c and CD1b were synthesized and coupled to sensor chips to study their interaction with purified AP-2 or AP-3 complexes using the BIAcore 3000 for SPR spectroscopy. The sequences of the tyrosine-based internalization motifs are underlined, and the residues mutated to alanines are shown in bold. (B) Sensorgrams of the interaction of wild-type CD1b.wt, CD1c.wt, TfR.wt and Lamp-1.wt tails, the mutant CD1b.Y>A, TfR.Y,F>A and Lamp-1.Y>A tails (mutant tails) or empty sensor chip (control) with purified AP-2 (left panel) or AP-3 (right panel) as measured by SPR. Note: the sensorgrams for the three mutant tails are overlapping with the sensorgram of the control for AP-2 and AP-3 measurements. (C) Affinities of the tail peptides for AP-2 (left) or AP-3 (right) are directly proportional to the inverse of the equilibrium dissociation constant ( $K_D$ ) shown in  $\mu\text{M}^{-1}$ . Asterisks indicate that binding of the TfR tail peptides was below the level of detection for the assay. Results shown are representative of three independent measurements, giving a standard deviation of between 3 and 7% of the  $K_D$  value.

CD1b to lysosomes and MIICs following its internalization from the PM, the interactions of purified AP-2 and AP-3 with the cytoplasmic tails of CD1b and several other proteins that localize within different levels of the endocytic system were analyzed using a biosensor system to monitor surface plasmon resonance (SPR). This technology has been used previously to study the interaction of cytoplasmic tail peptides with adaptor complexes (Boll *et al.*, 1995; Honing *et al.*, 1997). Interestingly, CD1b and CD1c tail peptides bound AP-2 with similar efficiencies, but only the CD1b wild-type tail bound AP-3 with higher affinity than the tyrosine-mutated control peptide (CD1b.Y311A) (Figure 5B).

Next the association of AP-2 and AP-3 with the tail of the lysosomal protein Lamp-1 was analyzed and compared with interactions with the tail of TfR, which accumulates only in early endosomes. Both molecules contain a tyrosine-based motif in their cytoplasmic tails (Kirchhausen *et al.*, 1997). The TfR tail peptide had the highest affinity for AP-2 as expressed in the equilibrium dissociation constant ( $K_D = 0.04 \mu\text{M}$ ), followed by the Lamp-1 tail ( $K_D = 0.12 \mu\text{M}$ ) and finally the CD1b and CD1c tails which had similar affinities ( $K_D = 0.35$  and  $0.29 \mu\text{M}$ , respectively) (Figure 5C and Table I). The specificity of the interaction was controlled using peptides with alanine mutations of the tyrosine residue of the

**Table I.** Overview of cytoplasmic tail peptide interactions with AP-2 or AP-3

Tail	AP-2			AP-3		
	$k_a$ (1/M×s)	$k_d$ (1/s)	$K_D$ (μM)	$k_a$ (1/M×s)	$k_d$ (1/s)	$K_D$ (μM)
CD1c wt	$1.9 \times 10^4$	$5.6 \times 10^{-3}$	0.29	$3.4 \times 10^2$	$4.7 \times 10^{-3}$	14.0
CDc1b wt	$1.4 \times 10^4$	$4.9 \times 10^{-3}$	0.35	$1.2 \times 10^3$	$4.2 \times 10^{-3}$	3.5
CDc1 Y>A	$1.2 \times 10^3$	$5.3 \times 10^{-3}$	4.4	$0.3 \times 10^3$	$4.0 \times 10^{-3}$	13.3
Lamp-1 wt	$2.6 \times 10^4$	$3.1 \times 10^{-3}$	0.12	$9.2 \times 10^2$	$3.4 \times 10^{-3}$	3.7
Lamp-1 Y>A	$8.7 \times 10^3$	$3.9 \times 10^{-3}$	4.5	$2.7 \times 10^2$	$3.9 \times 10^{-3}$	14.4
TfR wt	$1.2 \times 10^5$	$4.6 \times 10^{-3}$	0.04	nd <sup>a</sup>	nd	nd
TfR Y,F>A	$2.3 \times 10^3$	$5.2 \times 10^{-3}$	2.3	nd	nd	nd

The interaction of purified AP-2 and AP-3 complexes with cytoplasmic tail peptides was analyzed by SPR using a BIAcore 3000 as described in Materials and methods. The rate constants for association ( $k_a$ ) and dissociation ( $k_d$ ) were determined at three different concentrations of AP-2 and AP-3 for each peptide. Shown are the values measured with AP-2 and AP-3 at 500 nM. The equilibrium dissociation constant ( $K_D = k_d/k_a$ ) was calculated for each adaptor concentration. Values obtained from three independent sets of measurements varied by 3–7%.

<sup>a</sup>nd: not detectable.

YXXZ motif (Figure 5A), which all had significantly reduced affinity for AP-2 binding ( $K_D = 2.3$ – $4.5$  μM). In contrast, the affinity of the TfR tail peptide for AP-3 binding was not detectable, and instead the CD1b and Lamp-1 tail peptides both bound AP-3 with similar affinities ( $K_D = 3.5$  and  $3.7$  μM, respectively). The CD1c tail bound AP-3 only at the background level of the tyrosine-mutated peptides of CD1b or Lamp1 ( $K_D = 14.0$  μM) (Figure 5C and Table I). In conclusion, this analysis of direct binding by the biosensor system revealed a specific interaction of the cytoplasmic tail of the lysosomal proteins CD1b and Lamp-1 with the AP-3, but not of the early endosomal proteins CD1c and TfR, suggesting that AP-3 interaction may control the accumulation of CD1b in lysosomes.

#### **Requirement for *de novo* protein synthesis for efficient presentation of a microbial lipid by CD1b**

Studies on MHC class II molecules have demonstrated an alternative antigen presentation pathway for a small subset of peptide antigens that become associated with MHC class II through a recycling pathway (Pinet *et al.*, 1995). These studies have shown that using the irreversible protein synthesis inhibitor emetine, most MHC class II antigen presentation is prevented since traffic to the MIIC for antigen loading is dependent on *de novo* protein synthesis of both Ii and MHC class II  $\alpha$ - and  $\beta$ -chains. However, the alternative pathway is not blocked by emetine since it relies on the recycling of pre-existing MHC class II molecules from the cell surface and their loading with new peptide antigens that are presumably encountered during recycling through endosomes. Since CD1b may also have the potential to recycle from the PM, we used this experimental approach to assess if *de novo* CD1b synthesis was required for antigen presentation, or if a similar alternative pathway of antigen acquisition during recycling might also exist for CD1b.

Emetine treatment of the iDCs before addition of tetanus toxoid completely prevented T-cell recognition of this MHC class II-presented antigen, whereas treatment of iDCs after first pulsing them with tetanus toxoid had very little effect on subsequent presentation using the HLA-DR-restricted T-cell lines (SP-F3 and SP-F14) (Figure 6A). This was consistent with the ability of the iDCs to present this antigen only through *de novo* class II

synthesis as previously established for most exogenous protein antigens. Presentation of purified tetanus toxoid 15-mer peptides by cell surface MHC class II molecules of the iDCs was not affected by emetine treatment, as expected (data not shown). When the iDCs were tested for recognition of the CD1b-presented mycobacterial lipid antigens glucose mono-mycolate (GMM) or mycolic acid by CD1b-restricted T-cell lines specific for these antigens (LDN5 and DN1, respectively), results strikingly similar to those obtained for the MHC class II-presented antigens were observed. Thus, emetine treatment before antigen loading had a very strong inhibitory effect, whereas emetine treatment after antigen incubation did not inhibit antigen presentation mediated by CD1b (Figure 6B).

The similarity of the MHC class II- and CD1b-mediated antigen presentation prompted us to compare them with respect to the kinetics of antigen presentation at the cell surface. Thus, iDCs were pulsed with sonicated *M.tuberculosis* or with tetanus toxoid for various lengths of time at 37°C, fixed, and the presentation of either mycobacterial lipids by CD1b or tetanus toxoid peptides by MHC class II was analyzed by the proliferative response of specific T-cell lines (DN1 or SP-F14, respectively). This revealed that the kinetics of the MHC class II- and CD1b-mediated antigen presentation were almost identical (Figure 6C). In both cases, initial weak responses were barely detected after 15 min of incubation of the iDCs with the antigens, and then rose rapidly by 30 min to reach 60–80% of the maximal response, which was achieved in both cases by 60 min. These studies demonstrated surprising similarities at the functional level between the MHC class II-mediated antigen presentation of peptides and the CD1b-mediated lipid antigen presentation with respect to their dependence on *de novo* protein synthesis and their kinetics of antigen presentation at the cell surface.

## **Discussion**

CD1 molecules represent a third lineage of antigen-presenting molecules that are characterized by their ability to present lipid antigens (Porcelli, 1995). The steady-state intracellular distribution of the different human CD1 isoforms has been analyzed recently (for reviews see Briken *et al.*, 2000b; Jayawardena-Wolf and Bendelac,

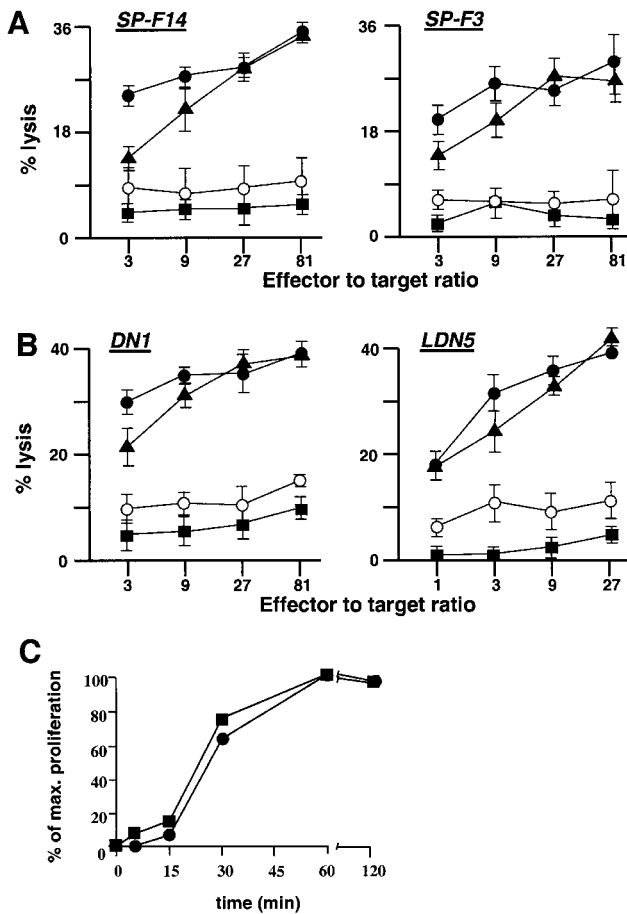


**Fig. 6.** Similar requirement for *de novo* protein synthesis for CD1b- and MHC class II-restricted antigen presentation. The requirement of MHC class II- (A) or CD1b- (B) restricted antigen presentation for *de novo* protein synthesis was assayed using iDCs as antigen-presenting cells. The iDCs were labeled with  $^{51}\text{Cr}$  and then split into four groups and treated as described in Materials and methods: antigen followed by emetine treatment (closed circles), emetine followed by antigen treatment (open circles), medium and emetine (squares) and, finally, medium and antigen treatment (triangles). These iDCs were used as target cells in a standard  $^{51}\text{Cr}$  release assay using the MHC class II-restricted, tetanus toxoid-specific T-cell clones SP-F14 and SP-F3, and the CD1b-restricted, mycolic acid-specific T-cell clone DN1 and GMM-specific LDN5. (C) The kinetics of lipid antigen presentation by CD1b (squares) or protein antigen presentation by MHC class II (circles) were compared. iDCs were incubated with antigen for the indicated times and the proliferative responses of the CD1b-restricted mycolic acid-specific T-cell line (DN1) or the MHC class II-restricted tetanus toxoid-specific T-cell line SP-F14 were determined. T-cell responses are represented as a percentage of the maximal response achieved for each T-cell line. For (A–C), the results shown are representative of three independent experiments.

2001); however, the intracellular transport pathways that CD1 molecules employ have not been elucidated. The current detailed study of the transport of newly synthesized CD1b molecules revealed that these molecules have evolved to follow an intracellular transport route ('out to the cell surface—into the endocytic pathway—back out to the cell surface') that is unlike the intracellular trafficking of MHC class I ('out to the cell surface') or the majority of MHC class II ('into the endocytic pathway—out to the cell surface') antigen-presenting molecules.

Our studies provided substantial insight into the molecular mechanisms that mediated the intracellular traf-

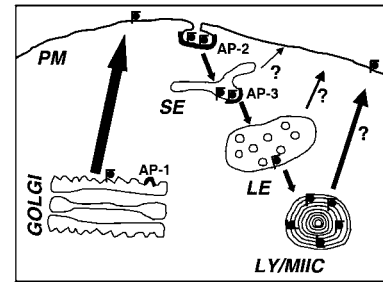


**Fig. 7.** Schematic representation of the intracellular trafficking of newly synthesized CD1b molecules. Newly synthesized CD1b molecules follow the secretory pathway for direct transport from the Golgi apparatus to the cell surface. The internalization of CD1b from the plasma membrane (PM) is mediated efficiently by AP-2 complexes. In the sorting endosomes (SE), CD1b molecules are sorted for transport into late endosomes (LE), instead of recycling to the PM. This sorting event may be mediated by the specific interaction of the CD1b tyrosine-based motif with AP-3 complexes. LE containing CD1b will eventually mature and fuse with lysosomes and/or MHC class II compartments (LY/MiIC), where CD1b molecules accumulate and associate with lipid antigens before they eventually reach the cell surface to present antigens to T cells. The recycling of CD1b from any compartment in the endocytic pathway to the cell surface has not been analyzed but since CD1b accumulates in LY/MiIC, the recycling from SE and LE is postulated to be inefficient.

fficking of CD1b. Biochemical analysis of the cell surface appearance of newly synthesized CD1b molecules clearly showed that once they reached the Golgi apparatus, they followed the secretory pathway with kinetics of transport to the cell surface that were very similar to those of proteins classically associated with this transport pathway, such as MHC class I or TfR molecules (Figures 2 and 7). Therefore, it was unlikely that CD1b molecules interacted with AP-1 complexes at the TGN, like MHC class II–Ii complexes, to induce sorting into the endocytic pathway (Figure 7). Once at the cell surface, CD1b molecules were internalized through a mechanism that was mediated by the AP-2 complex. This conclusion was supported by overexpression of dominant-negative dynamin mutants that induced a redistribution of CD1b and the TfR to the cell surface. In contrast, the intracellular distributions of HLA-DM and Lamp-1, both proteins that are sorted mainly at the TGN through interactions with AP-1, were not affected (Figure 4B and C). In addition, the cytoplasmic tail of CD1b specifically bound purified AP-2 complexes in assays carried out using the Biacore biosensor to measure SPR signals generated by this interaction (Figure 5 and Table I).

Taken together, our analysis indicated that after internalization from the PM, CD1b molecules were sorted for transport to lysosomes in the sorting endosome (SE), whereas molecules like TfR or CD1c recycled to the PM (Figure 7). The AP-3 complex is localized on TGN and endosomes and is implicated in biosynthetic transport of proteins from the TGN to lysosomes and the formation of synaptic vesicles from endosomes (Dell'Angelica *et al.*, 1997, 1999; Faundez *et al.*, 1998). In the first biochemical analysis to date to study the interaction of purified AP-3 complexes with cytoplasmic tail peptides, we demonstrated a specific affinity of the cytoplasmic tails of the two lysosomal proteins Lamp-1 and CD1b, but not of the early endosomal proteins TfR and CD1c, for the AP-3 complex (Figure 5 and Table I). These results were consistent with

the finding that Lamp-1 but not the TfR YXXZ motif can bind the AP-3  $\mu$ -chain in yeast two-hybrid analyses (Dell'Angelica *et al.*, 1999). Overall, our data strongly suggested that the main fraction of newly synthesized CD1b molecules was sorted for rapid transport to the PM in the TGN, which excluded interaction of CD1b with AP-3 at this site. The question arises of why, according to our model, CD1b molecules interacted with AP-3 on endosomes but not in the TGN. The affinities of Lamp-1 and CD1b for AP-3, although significantly above background, were  $\sim 10$ -fold lower than their affinities for AP-2 complexes. Therefore, the relatively weak interaction with AP-3 may not allow efficient sorting of CD1b at the TGN, but could be strong enough to account for the sorting in endosomes, since molecules that escaped a first interaction in the SE would recycle to the PM and be internalized to allow for a second chance to interact with AP-3, and so on. These repeated interactions may therefore account for a net accumulation of the molecules in lysosomes. Alternatively, it is possible that *in vivo* other structural elements in the membranes of the SE but not the TGN stabilize the interaction of CD1b with AP-3, such as the amount of phosphatidylinositol phosphates which are known to regulate the affinity of AP-2 for YXXZ motifs (Rapoport *et al.*, 1997). Altogether, these data indicate that the AP-3 complex may mediate the sorting of CD1b and Lamp-1 molecules in endosomes for transport to lysosomes, although *in vivo* studies are needed to determine definitively the function of AP-3 in the sorting of CD1b for lysosomal transport.

The most prominent known function of CD1b molecules is to associate with lipids from pathogens in order to stimulate T cells and induce host defense mechanisms. Thus, it is interesting to speculate on how the intracellular transport pathway adapted by newly synthesized CD1b may provide an advantage for their function in the presentation of antigenic lipids. The importance of the pool of nascent CD1b molecules for the presentation of at least two microbial lipids was demonstrated by functional studies using the drug emetine to inhibit *de novo* protein synthesis. This revealed that antigen presentation of GMM and mycolic acid by CD1b was sensitive to inhibition of protein synthesis, behaving similarly in this regard to the presentation of a protein-derived epitope by MHC class II (Figure 6). In the case of MHC class I and class II molecules, complex intracellular mechanisms lead to the accumulation of the majority of antigenic peptides in distinct compartments, ER and lysosomes, respectively. In contrast, for antigenic lipids, such mechanisms may not exist as lipids may distribute throughout the cell according to the composition of their alkyl chains (Mukherjee *et al.*, 1999). This has been demonstrated in cells infected with intracellular pathogens such as *M.tuberculosis*, in which bacterial lipids are shed from the phagosome and distribute throughout the endocytic pathway (Beatty *et al.*, 2000; Schaible *et al.*, 2000). Consequently, the transport pathway of newly synthesized CD1b ('out-in-out') has the advantage of allowing CD1b to sample lipids in a wider variety of intracellular compartments. In contradiction to this hypothesis is the finding that CD1b requires an acidic pH for the association with certain bacterial lipid antigens such as mycolic acids, LAM and GMM, suggesting that lipid loading only takes place in late endosomes or

lysosomes (Porcelli *et al.*, 1992; Ernst *et al.*, 1998). However, more recent work now shows that association of CD1b with GMMs from other bacterial strains, that are characterized by shorter alkyl chains, or with endogenous lipids such as gangliosides, can take place efficiently at neutral pH at the PM (D.B.Moody and S.A.Porcelli, unpublished results; Shamshiev *et al.*, 2000). Thus, the low pH of late endosomes may not be an absolute requirement for all CD1b-mediated antigen presentation.

In conclusion, newly synthesized MHC class I and class II have evolved intracellular trafficking pathways that are most suitable for their function in capturing and presenting antigenic peptides in the ER and lysosomes, respectively. The current study represents, to our knowledge, the first extensive analysis of the intracellular trafficking of one human CD1 isoform. Our findings revealed that CD1b followed an intracellular transport pathway that led first to the cell surface after synthesis in the ER, and then subsequently to internalization from the PM into the endocytic pathway followed by re-expression on the cell surface. We speculate that this transport pathway allows newly synthesized CD1b molecules to sample the lipid content of a great variety of intracellular compartments, and may therefore represent an important adaptation to their function in the presentation of antigenic lipids.

## Materials and methods

### Cell lines and antibodies

The lipid antigen-specific T-cell lines DN1 (Porcelli *et al.*, 1992) and LDN5 (Moody *et al.*, 1997) and the tetanus toxoid-specific T-cell lines SP-F14 and SP-F3 (Roncarolo *et al.*, 1988) have been described. *In vitro*-derived immature dendritic cells were prepared as described (Beckman *et al.*, 1996). The CD1b-transfected B-lymphoma cell line C1R has been described and the HLA-A3-transfected C1R cells were a kind gift of Dr P.Cresswell (Storkus *et al.*, 1989). HeLa cells containing stably transfected and tetracycline-repressible dominant-negative mutants (K44A and G273D) of dynamin (Damke *et al.*, 1995a,b) were provided by Dr S.L.Schmid.

The following antibodies and antisera were used: 4A7.6 (anti-CD1b; Olive *et al.*, 1984), BCD1b3.1 (anti-CD1b; Behar *et al.*, 1995), 5E9 (anti-transferrin; Haynes *et al.*, 1981), GAP-A3 (anti-HLA-A3; Storkus *et al.*, 1989), W6/32 (anti HLA-A, -B, -C; Brodsky and Parham, 1982), DA6.147 (anti HLA-DR; Guy *et al.*, 1982), L243 (anti HLA-DR; Lampson and Levy, 1980), P3 [isotype control for IgG1; American Type Culture Collection (ATCC), Manassas, VA], RPC5.4 (isotype control for IgG2a; ATCC), rabbit anti-human Lamp-1 antiserum (Carlsson *et al.*, 1988), rabbit anti-human CD1b antiserum (Sugita *et al.*, 1997) and rabbit anti-HLA-DM $\beta$  (Denzin *et al.*, 1994). The secondary antibodies Cy2/Cy3-conjugated donkey anti-mouse or donkey anti-rabbit were purchased from Jackson Research Laboratories (West Grove, PA). Horseradish peroxidase (HRP)-conjugated goat anti-rabbit IgG was purchased from Zymed (San Francisco, CA).

### Immunofluorescence and confocal microscopy

Immature DCs and C1R cells were attached to poly-L-lysine-coated coverslips, fixed in 2% paraformaldehyde and permeabilized in 0.05% saponin as described (Briken *et al.*, 2000a). Cells were stained with the primary and secondary antibodies for 30 min each and finally mounted in ProLong™ Antifade Reagent Kit (Molecular Probes, Eugene, OR) and analyzed by confocal microscopy.

### Surface plasmon resonance spectroscopy

AP-2 and AP-3 complexes were purified from pig brain or bovine brain and assessed for purity according to previously published methods (Honing *et al.*, 1997; Faundez *et al.*, 1998). The cytoplasmic tail peptides for Lamp-1 and TfR were synthesized, purified and coupled to CM5 sensor chips as described (Honing *et al.*, 1997, 1998). The CD1b and CD1c tail peptides were synthesized with an N-terminal biotin residue at the Albert Einstein College of Medicine core facility and purified by HPLC. Purity was confirmed using UV spectrometry and mass

spectrometry. These peptides were bound to streptavidin-coated SA5 sensor chips. All interaction experiments were performed using the BIAcore 3000 biosensor for measurement of SPR as described (Honing *et al.*, 1997, 1998). AP2 and AP3 were used at final protein concentrations ranging from 50 to 750 nM. Kinetic parameters and equilibrium dissociation constants were determined from sensorgrams recorded at different adaptor concentrations using the evaluation software of the BIAcore 3000 according to previously published methods (Honing *et al.*, 1997, 1998).

#### Subcellular fractionation and western blotting

The fractionation of iDCs and C1R cells was performed as previously described (Briken *et al.*, 2000a). Briefly,  $3 \times 10^7$  cells were taken up in 1 ml of homogenization buffer, passed through a ball-bearing homogenizer and the post-nuclear supernatant was applied to a 25% Percoll gradient. Twelve fractions were collected and assayed for the lysosomal and plasma membrane marker enzymes,  $\beta$ -hexosaminidase (B-Hex) and alkaline phosphodiesterase (APDE), respectively. The relative distribution of CD1b in each gradient was determined by western immunoblotting using the rabbit anti-CD1b antiserum as described (Briken *et al.*, 2000a) followed by quantification of the signal by densitometry using the ScionImage software (NIH).

#### Dynamin mutant assay

HeLa cells stably expressing the K44A-dynamin mutant were transiently transfected with 1.5  $\mu$ g of CD1b plasmid (pSR $\alpha$ NEO-CD1b) or plasmids coding for the HLA-DM  $\alpha$ - and  $\beta$ -chains (Denzin *et al.*, 1994) using the Superfect<sup>TM</sup> lipid reagent (Qiagen Corp., Valencia, CA) following the manufacturer's instructions. Cells were then either left in tetracycline-containing medium or shifted to tetracycline-free medium to induce the expression of K44A-dynamin. After 48 h, the distribution of CD1b, HLA-DM and TfR was analyzed in the cells kept in Tet<sup>+</sup> or Tet<sup>-</sup> medium by immunofluorescence microscopy as previously described (Jackman *et al.*, 1998). Alternatively, HeLa cells expressing the temperature-sensitive, dominant-negative G273D-dynamin mutant were stably transfected with the CD1b cDNA in the expression vector p3-9 (gift of Dr L.Glimcher, Harvard Medical School, Boston, MA) using CaPO<sub>4</sub> precipitation as described (Jackman *et al.*, 1998). CD1b-expressing cells were selected in 200  $\mu$ g/ml hygromycin B. Cells expressing high levels of CD1b were collected by fluorescence-activated cell sorting (FACS) and used for the experiments.

#### Internalization assays

In order to determine the kinetics of cell surface internalization of TfR, MHC class I and CD1b,  $4 \times 10^7$  CD1b-transfected C1R cells were biotinylated using a reactive form of biotin containing a cleavable disulfide bond (Sulfo-NHS-SS-biotin; Pierce, Rockford, IL) as described (Briken *et al.*, 1997) and then split into equal aliquots and incubated at 37°C for various times or left at 4°C. The cell surface biotin was cleaved using the reducing agent 2-mercaptoethanesulfonic acid (MESNA) (20 mM MESNA, 50 mM Tris pH 8.6, 100 mM NaCl, 0.2% bovine serum albumin) at 4°C for 15 min twice. Cells were lysed using 0.5% Triton X-100 and the amount of biotinylated proteins protected from the MESNA treatment was determined by capture enzyme-linked immunosorbent assay (ELISA).

For the end point internalization assay, C1R cells were incubated with the primary antibodies (W6/32, 5E9 and 4A7.6) for 60 min on ice, washed with phosphate-buffered saline (PBS) and incubated for an additional 45 min with <sup>125</sup>I-labeled rabbit anti-mouse IgG. After washing with PBS, cells were either left on ice or incubated at 37°C for 75 min. Cells were split in two, to be washed with either PBS or a solution of 0.25 M NaCl/0.25 M acetic acid pH 2.1 (elution wash) on ice. After 10 min, cells were washed with PBS and the amount of associated radioactivity was determined by a  $\gamma$ -counter (Beckman Instruments, Inc., Fullerton, CA). Internalization was determined by the formula  $(X - n)/(Y - n)$  where  $X$  is the acid-resistant counts at time  $t$ ,  $Y$  is the total cell-associated counts (PBS wash) at time  $t$ , and  $n$  is the non-specific cell-associated <sup>125</sup>I that was resistant to acid wash at time 0.

#### Metabolic labeling and immunoprecipitation

For metabolic labeling,  $5 \times 10^8$  C1R cells, expressing either CD1b or HLA-A3, were labeled with [<sup>35</sup>S]methionine/cysteine, chased for various times at 37°C, and subsequently cell surface proteins were biotinylated as described (Briken *et al.*, 1997). Cells were lysed in 0.5% Triton X-100, and immunoprecipitations using specific monoclonal antibodies for CD1b (BCD1b3.1), HLA-A3 (GAP-A3), MHC class II (mixture of DA6.147 and L243), TfR (5E9) or isotype control antibodies (P3 and RPC5.4) were performed. The precipitated proteins were eluted from the washed and

dried Sepharose beads by boiling in 100  $\mu$ l of 2% SDS/PBS for 5 min. A 90  $\mu$ l aliquot of the eluate was diluted in 1 ml of lysis buffer, and streptavidin-agarose (Pierce, Chemical Co., Rockford, IL) was added for 2 h at 4°C to immunoprecipitate biotinylated proteins. The washed and dried streptavidin-beads and the remaining 10  $\mu$ l of eluate of the first immunoprecipitation were subjected to EndoH digestion for 5–16 h in EndoH buffer (100 mM sodium citrate pH 5.5, 0.2% SDS) using 5 mU of EndoH (Boehringer Mannheim, Mannheim, Germany) per point. Samples were boiled, reduced and separated by SDS-PAGE. Dried gels were exposed to MR films and intensifying screens (Eastman Kodak Co.) at -80°C. Signals were quantified either by densitometry using the ScionImage software (NIH) or by PhosphorImager (Molecular Dynamics, Sunnyvale, CA) using the ImageQuant<sup>TM</sup> software.

#### Antigen presentation

To test the requirement for *de novo* protein synthesis of MHC class II- or CD1b-restricted antigen presentation, iDCs were labeled with <sup>51</sup>Cr as described (Porcelli *et al.*, 1992) and then split into four groups. The first group was incubated for 8.5 h with antigen (1  $\mu$ g/ml of intact tetanus toxoid and 1  $\mu$ g/ml of GMM or 5  $\mu$ g/ml of mycolic acid), then washed, followed by a 8.5 h incubation with 20  $\mu$ M emetine. The second group was first treated with emetine, washed and then incubated with antigen. The third group was incubated in medium, washed and treated with emetine. The last group was incubated in medium, washed and then incubated with antigen. These four different groups of samples were rinsed twice in PBS and a standard <sup>51</sup>Cr release cytolytic assay was performed in triplicate using the MHC class II-restricted T-cell clones SP-F14 or SP-F3, the CD1b-restricted GMM-specific T-cell line LDN5 or the mycolic acid-specific T-cell line DN1 in different effector to target ratios (Porcelli *et al.*, 1992).

Determination of the kinetics of antigen presentation by CD1b in comparison with MHC class II was done using T-cell proliferative responses as the readout for T-cell activation. Immature DCs were pulsed with 10  $\mu$ g/ml of crude *M.tuberculosis* extract or 10  $\mu$ g/ml of tetanus toxoid for various times at 37°C, and then placed on ice. The antigen-pulsed iDCs were then fixed using 0.0125% glutaraldehyde in PBS for 30 s at room temperature, followed by quenching of the fixative with 0.2 M L-lysine in water. The antigen-pulsed and fixed APCs were then cultured in triplicate in 96-well plate wells with the appropriate antigen-specific T cells. The cultures were incubated at 37°C for 42 h, pulsed with 1  $\mu$ Ci/well of [<sup>3</sup>H]thymidine (New England Nuclear) for 6 h, and then harvested and processed for  $\beta$ -scintillation counting to determine the incorporation of [<sup>3</sup>H]thymidine.

#### Acknowledgements

We would like to thank the Drs S.L.Schmid, P.Cresswell and M.Fukuda for gifts of reagents. V.B. is the recipient of a long-term fellowship from the Human Frontiers Science Program. S.D. is the recipient of a National Science Foundation predoctoral fellowship. S.H. is supported by a grant of the German Science Foundation (SFB523/A5). S.A.P. is supported by grants from the NIAID (AI45889 and AI48933) and is the recipient of an award from the Irene Diamond Foundation.

#### References

- Beatty,W.L., Rhoades,E.R., Ullrich,H.J., Chatterjee,D., Heuser,J. and Russell,D.G. (2000) Trafficking and release of mycobacterial lipids from infected macrophages. *Traffic*, **1**, 235–247.
- Beckman,E.M. *et al.* (1996) CD1c restricts responses of mycobacteria-specific T cells. Evidence for antigen presentation by a second member of the human CD1 family. *J. Immunol.*, **157**, 2795–2803.
- Behar,S.M., Porcelli,S.A., Beckman,E.M. and Brenner,M.B. (1995) A pathway of costimulation that prevents anergy in CD28-T cells: B7-independent costimulation of CD1-restricted T cells. *J. Exp. Med.*, **182**, 2007–2018.
- Boll,W., Gallusser,A. and Kirchhausen,T. (1995) Role of the regulatory domain of the EGF-receptor cytoplasmic tail in selective binding of the clathrin-associated complex AP-2. *Curr. Biol.*, **5**, 1168–1178.
- Bonifacino,J.S. and Dell'Angelica,E.C. (1999) Molecular bases for the recognition of tyrosine-based sorting signals. *J. Cell Biol.*, **145**, 923–926.
- Bonifacino,J.S., Marks,M.S., Ohno,H. and Kirchhausen,T. (1996) Mechanisms of signal-mediated protein sorting in the endocytic and secretory pathways. *Proc. Assoc. Am. Phys.*, **108**, 285–295.
- Briken,V., Lankar,D. and Bonnerot,C. (1997) New evidence for two

- MHC class II-restricted antigen presentation pathways by overexpression of a small G protein. *J. Immunol.*, **159**, 4653–4658.
- Briken, V., Jackman, R.M., Watts, G.F., Rogers, R.A. and Porcelli, S.A. (2000a) Human CD1b and CD1c isoforms survey different intracellular compartments for the presentation of microbial lipid antigens. *J. Exp. Med.*, **192**, 281–288.
- Briken, V., Moody, D.B. and Porcelli, S.A. (2000b) Diversification of CD1 proteins: sampling the lipid content of different cellular compartments. *Semin. Immunol.*, **12**, 517–525.
- Brodsky, F.M. and Parham, P. (1982) Monomorphic anti-HLA-A,B,C monoclonal antibodies detecting molecular subunits and combinatorial determinants. *J. Immunol.*, **128**, 129–135.
- Burdin, N. and Kronenberg, M. (1999) CD1-mediated immune responses to glycolipids. *Curr. Opin. Immunol.*, **11**, 326–331.
- Carlsson, S.R., Roth, J., Piller, F. and Fukuda, M. (1988) Isolation and characterization of human lysosomal membrane glycoproteins, h-lamp-1 and h-lamp-2. Major sialoglycoproteins carrying polylectosaminoglycan. *J. Biol. Chem.*, **263**, 18911–18919.
- Chiu, Y.H., Jayawardena, J., Weiss, A., Lee, D., Park, S.H., Dautry-Varsat, A. and Bendelac, A. (1999) Distinct subsets of CD1d-restricted T cells recognize self-antigens loaded in different cellular compartments. *J. Exp. Med.*, **189**, 103–110.
- Damke, H., Baba, T., Warnock, D.E. and Schmid, S.L. (1994) Induction of mutant dynamin specifically blocks endocytic coated vesicle formation. *J. Cell Biol.*, **127**, 915–934.
- Damke, H., Gossen, M., Freundlieb, S., Bujard, H. and Schmid, S.L. (1995a) Tightly regulated and inducible expression of dominant interfering dynamin mutant in stably transformed HeLa cells. *Methods Enzymol.*, **257**, 209–220.
- Damke, H., Baba, T., van der Blik, A.M. and Schmid, S.L. (1995b) Clathrin-independent pinocytosis is induced in cells overexpressing a temperature-sensitive mutant of dynamin. *J. Cell Biol.*, **131**, 69–80.
- Dell'Angelica, E.C., Ohno, H., Ooi, C.E., Rabinovich, E., Roche, K.W. and Bonifacio, J.S. (1997) AP-3: an adaptor-like protein complex with ubiquitous expression. *EMBO J.*, **16**, 917–928.
- Dell'Angelica, E.C., Shotelersuk, V., Aguilar, R.C., Gahl, W.A. and Bonifacio, J.S. (1999) Altered trafficking of lysosomal proteins in Hermansky-Pudlak syndrome due to mutations in the  $\beta$ 3A subunit of the AP-3 adaptor. *Mol. Cell*, **3**, 11–21.
- Denzin, L.K., Robbins, N.F., Carboy-Newcomb, C. and Cresswell, P. (1994) Assembly and intracellular transport of HLA-DM and correction of the class II antigen-processing defect in T2 cells. *Immunity*, **1**, 595–606.
- Ernst, W.A. *et al.* (1998) Molecular interaction of CD1b with lipoglycan antigens. *Immunity*, **8**, 331–340.
- Faundez, V., Horng, J.T. and Kelly, R.B. (1998) A function for the AP3 coat complex in synaptic vesicle formation from endosomes. *Cell*, **93**, 423–432.
- Germain, R.N. and Margulies, D.H. (1993) The biochemistry and cell biology of antigen processing and presentation. *Annu. Rev. Immunol.*, **11**, 403–450.
- Guy, K., Van, H., V, Cohen, B.B., Deane, D.L. and Steel, C.M. (1982) Differential expression and serologically distinct subpopulations of human Ia antigens detected with monoclonal antibodies to Ia  $\alpha$  and  $\beta$  chains. *Eur. J. Immunol.*, **12**, 942–948.
- Haynes, B.F., Hemler, M., Cotner, T., Mann, D.L., Eisenbarth, G.S., Strominger, J.L. and Fauci, A.S. (1981) Characterization of a monoclonal antibody (5E9) that defines a human cell surface antigen of cell activation. *J. Immunol.*, **127**, 347–351.
- Heemels, M.T. and Ploegh, H. (1995) Generation, translocation and presentation of MHC class I-restricted peptides. *Annu. Rev. Biochem.*, **64**, 463–491.
- Honing, S., Sosa, M., Hille-Rehfeld, A. and von Figura, K. (1997) The 46-kDa mannose 6-phosphate receptor contains multiple binding sites for clathrin adaptors. *J. Biol. Chem.*, **272**, 19884–19890.
- Honing, S., Sandoval, I.V. and von Figura, K. (1998) A di-leucine-based motif in the cytoplasmic tail of LIMP-II and tyrosinase mediates selective binding of AP-3. *EMBO J.*, **17**, 1304–1314.
- Jackman, R.M. *et al.* (1998) The tyrosine-containing cytoplasmic tail of CD1b is essential for its efficient presentation of bacterial lipid antigens. *Immunity*, **8**, 341–351.
- Jayawardena-Wolf, J. and Bendelac, A. (2001) CD1 and lipid antigens: intracellular pathways for antigen presentation. *Curr. Opin. Immunol.*, **13**, 109–113.
- Kirchhausen, T., Bonifacio, J.S. and Riezman, H. (1997) Linking cargo to vesicle formation: receptor tail interactions with coat proteins. *Curr. Opin. Cell Biol.*, **9**, 488–495.
- Lampson, L.A. and Levy, R. (1980) Two populations of Ia-like molecules on a human B cell line. *J. Immunol.*, **125**, 293–299.
- Mellman, I., Pierre, P. and Amigorena, S. (1995) Lonely MHC molecules seeking immunogenic peptides for meaningful relationships. *Curr. Opin. Cell Biol.*, **7**, 564–572.
- Moody, D.B. *et al.* (1997) Structural requirements for glycolipid antigen recognition by CD1b-restricted T cells. *Science*, **278**, 283–286.
- Moody, D.B. *et al.* (2000) CD1c-mediated T cell recognition of isoprenoid glycolipids in *M. tuberculosis* infection. *Nature*, **404**, 884–888.
- Mukherjee, S., Soe, T.T. and Maxfield, F.R. (1999) Endocytic sorting of lipid analogues differing solely in the chemistry of their hydrophobic tails. *J. Cell Biol.*, **144**, 1271–1284.
- Neefjes, J.J., Stollorz, V., Peters, P.J., Geuze, H.J. and Ploegh, H.L. (1990) The biosynthetic pathway of MHC class II but not class I molecules intersects the endocytic route. *Cell*, **61**, 171–183.
- Olive, D., Dubreuil, P. and Mawas, C. (1984) Two distinct TL-like molecular subsets defined by monoclonal antibodies on the surface of human thymocytes with different expression on leukemia lines. *Immunogenetics*, **20**, 253–264.
- Pamer, E. and Cresswell, P. (1998) Mechanisms of MHC class I-restricted antigen processing. *Annu. Rev. Immunol.*, **16**, 323–358.
- Pieters, J. (1997) MHC class II restricted antigen presentation. *Curr. Opin. Immunol.*, **9**, 89–96.
- Pinet, V., Vergelli, M., Martin, R., Bakke, O. and Long, E.O. (1995) Antigen presentation mediated by recycling of surface HLA-DR molecules. *Nature*, **375**, 603–606.
- Porcelli, S.A. (1995) The CD1 family: a third lineage of antigen-presenting molecules. *Adv. Immunol.*, **59**, 1–98.
- Porcelli, S.A. and Modlin, R.L. (1999) The CD1 system: antigen-presenting molecules for T cell recognition of lipids and glycolipids. *Annu. Rev. Immunol.*, **17**, 297–329.
- Porcelli, S., Morita, C.T. and Brenner, M.B. (1992) CD1b restricts the response of human CD4(–)8(–) T lymphocytes to a microbial antigen. *Nature*, **360**, 593–597.
- Rapoport, I., Miyazaki, M., Boll, W., Duckworth, B., Cantley, L.C., Shoelson, S. and Kirchhausen, T. (1997) Regulatory interactions in the recognition of endocytic sorting signals by AP-2 complexes. *EMBO J.*, **16**, 2240–2250.
- Roncarolo, M.G., Yssel, H., Touraine, J.L., Bacchetta, R., Gebuhrer, L., de Vries, J.E. and Spits, H. (1988) Antigen recognition by MHC-incompatible cells of a human mismatched chimera. *J. Exp. Med.*, **168**, 2139–2152.
- Salem, N., Faundez, V., Horng, J.T. and Kelly, R.B. (1998) A v-SNARE participates in synaptic vesicle formation mediated by the AP3 adaptor complex. *Nature Neurosci.*, **1**, 551–556.
- Schaible, U.E., Hagens, K., Fischer, K., Collins, H.L. and Kaufmann, S.H.E. (2000) Intersection of group ICD1 molecules and mycobacteria in different intracellular compartments of dendritic cells. *J. Immunol.*, **164**, 4843–4852.
- Schmid, S.L. (1997) Clathrin-coated vesicle formation and protein sorting: an integrated process. *Annu. Rev. Biochem.*, **66**, 511–548.
- Shamshiev, A. *et al.* (2000) The  $\alpha\beta$  T cell response to self-glycolipids shows a novel mechanism of CD1b loading and a requirement for complex oligosaccharides. *Immunity*, **13**, 255–264.
- Simpson, F., Peden, A.A., Christopoulou, L. and Robinson, M.S. (1997) Characterization of the adaptor-related protein complex, AP-3. *J. Cell Biol.*, **137**, 835–845.
- Storkus, W.J., Alexander, J., Payne, J.A., Dawson, J.R. and Cresswell, P. (1989) Reversal of natural killing susceptibility in target cells expressing transfected class I HLA genes. *Proc. Natl Acad. Sci. USA*, **86**, 2361–2364.
- Sugita, M., Jackman, R.M., van Donselaar, E., Behar, S.M., Rogers, R.A., Peters, P.J., Brenner, M.B. and Porcelli, S.A. (1996) Cytoplasmic tail-dependent localization of CD1b antigen-presenting molecules to MHCs. *Science*, **273**, 349–352.
- Sugita, M., Porcelli, S.A. and Brenner, M.B. (1997) Assembly and retention of CD1b heavy chains in the endoplasmic reticulum. *J. Immunol.*, **159**, 2358–2365.
- Sugita, M., Grant, E.P., van Donselaar, E., Hsu, V.W., Rogers, R.A., Peters, P.J. and Brenner, M.B. (1999) Separate pathways for antigen presentation by CD1 molecules. *Immunity*, **11**, 743–752.

Received September 28, 2001; revised December 17, 2001;  
accepted January 4, 2002